Proc. VIIth Digital Image Computing: Techniques and Applications, Sun C., Talbot H., Ourselin S. and Adriaansen T. (Eds.), 10-12 Dec. 2003, Sydney

Isotropic Subpixel Measurement of Circular Objects

Russell B Horney, Imants D Svalbe, Peter Wells

Monash University, Wellington Road, Clayton, Victoria, Australia
Russell.Horney@spme.monash.edu.au

Abstract. Many industrial manufacturing processes depend on the rapid and accurate measurement of circular objects, for example, pipe, tube and ball and roller bearings, to ensure that the components satisfy the engineering tolerance standards. Despite the importance of these measurements, they are often carried out using time-consuming, manual and randomly sampled procedures. Cross-sectional imaging techniques offer the advantage of simultaneous dense measurement of dimensions and the detection of defects. Levels of precision achievable using x-ray computed tomography (CT) to measure circular objects are determined here. Edge detection procedures have achieved subpixel measurement to a precision of 3.5 x 10^{-2} pixels (17 microns) using a medical x-ray CT scanner. Even when the image function is properly sampled and the image is a perfect isotropic disc, it is possible for significant anisotropic effects to be introduced when sampled data is processed. Methods of overcoming such effects are described as are techniques for handling image noise.

1 Introduction

Many industrial manufacturing processes depend on the accurate measurement of circular shapes. For example, in pipe or tube manufacture, it is necessary to maintain parameters such as inside diameter, outside diameter, wall thickness, ovality and eccentricity within tolerances specified by the manufacturing standards. The measurements required to control these parameters are often time consuming. For example, in preparing for a mill run to manufacture stainless steel tube, many lengths of tube are wasted as a tube is pressed, measurements made manually using micrometers, the mill adjusted and the cycle repeated until the specified tolerances are achieved. Even if mill set-ups from a previous run are used as a starting point, this process can take a considerable amount of time.

It may be possible to make such processes more efficient using an automated cross-sectional imaging technique. Apart from the fact that all of the relevant dimensional parameters could be obtained at once using such a process, additional information could be obtained at the same time. For example, in the manufacture of copper tube, it is important to know whether any damage in the form of line defects has occurred during pressing. Also, in the manufacture of food or pharmaceutical grade stainless steel welded tube, no weld undercut is permitted on the inside of the tube (to eliminate cavities in which bacteria could grow).

Various experimental methods for the measurement of circular objects are in use. Ultrasonic pulse-echo techniques are used to monitor dimensions of plastic medical tube during manufacture and feedback control of tube dimensions is possible [1]. However, contact with the object is required and accuracy may be affected by temperature. Pipes have been measured using a single x-ray CT projection replicated to form an image [2] but the method assumes that the pipe is circular, therefore it cannot be used to measure circumferentially varying parameters. This work is part of a larger study to determine whether circular objects may be measured using x-ray CT methods with sufficient precision to satisfy required standards. Using the techniques described below, a medical x-ray CT scanner has been used to make a preliminary measurement of the diameter of a circular object to a precision of 3.5 x 10^{-2} pixels or 17 microns, while the nominal resolution of the system is only 0.5 mm. To our knowledge, measurement of a disc to this precision using a medical scanner has not been reported.

In making accurate dimensional measurements of objects from digital images it is necessary to ensure that the input data sampling rate is adequate to avoid distortion of information when the digital image array is interpreted. However, it is possible for significant anisotropic effects to arise even when the analog data is properly sampled. Our present purpose is to show

1. How such anisotropic effects may arise when taking measurements from properly sampled digital images,
2. How it is possible to obtain virtually isotropic subpixel measurements from properly sampled, computer-generated discs, and
3. That the technique described is applicable to computer generated disc images with noise added and experimental data from x-ray CT images.

Measurements of the dimensions of circular objects depend on accurate detection and localisation of edges in the image. Many methods of edge detection have been reported in the literature [3]. The principal methods include: detection of the maximum of the first derivative in the image, detection of the zero-crossing of the second derivative, probabilistic methods and wavelet methods. Most edge detection methods are applied to complex images such as natural scenes, where a precision of one pixel is often suffiecient but the present application requires accurate subpixel location of the edge. A number of authors have considered edge location to subpixel accuracy [4] [5] [6] but few have studied accurate edge location in approximately circular objects. Chen and Lin [7] described an orthogonal circular detector which uses orthogonal, 9 x 9 masks representing a circular detecting area to determine the edge points of a circular object. While this method has good subpixel accuracy, it is based on the assumption that the object detected is circular. Since the purpose of the present work is to measure possibly deformed circular objects, circularity may not be assumed in this case. Van Vliet [8] and Verbeek and van Vliet [9] investigated the systematic errors introduced into various circular edge location methods and also the effects of noise in the data, and much of this work is based on their methods and results.

The paper is structured as follows. Section 2 describes the medical CT scanner on which the x-ray experiments were carried out and the method of com-

puter generation of disc images for testing the edge detection program. Section 3 outlines the edge detection procedure used. Section 4 describes the patch-circle centreline method of zero-crossing detection and noise-free results. Section 5 discusses the results of the noise-containing measurements obtained and methods used to ameliorate the effects of noise in the data used for those tests.

2 Experimental

2.1 Medical Scanner

X-ray data were acquired using an Hitachi W1000, third generation, medical CT scanner. A 230 mm diameter cylindrical polyethylene test object (a calibration phantom) with a thickness of 40 mm was used for these preliminary experiments. The same protocol was used for each scan and parameters were selected to keep image noise as low as possible. They were: tube voltage, 120 kV; tube current, 250 mA; scan time, 3.8 s; slice thickness, 10 mm; and scanned array size, 512 x 512 pixels.

2.2 Computer Generated Test Discs

Computer generated test discs were required to assess accurately the performance of the edge detection procedure. Discs were generated directly in the Fourier (spatial frequency) domain using a Bessel function of the first kind to represent the profile of the 2-dimensional Fourier transform of a perfect disc. This profile function was band-limited for proper sampling by applying a Gaussian filter of size σ, truncated at a radius of $a\sigma$, where a is the truncation factor. The expression for the profile, H_{2D}, of the Fourier transform is [8]

$$H_{2D} = \frac{2}{\pi} \int \sqrt{1-\zeta^2} e^{-2\pi\zeta\upsilon} d\zeta = \frac{J_1\big(2\pi\upsilon\big)}{\pi\upsilon} \tag{1}$$

where υ is the spatial frequency variable.

The Fourier transform of a disc of any given size was produced by scaling the frequencies to the radius of the disc to be generated. In this way, a synthetic 'perfect' disc of 235 pixels radius was generated to match the size, in pixels, of the CT test object to be measured.

2.3 Addition of Noise to Computer Generated Discs

To investigate the effects of noise on the edge location procedure, random Gaussian noise with approximately the same standard deviation as the noise in a real CT image was added to the disc directly in the Fourier domain. The noise level in the real CT image was measured over a circular region about the centre of the disc image.

3 Edge Detection Procedure

The detection process used here is based on finding the zero-crossing of the second derivative of the image in the gradient direction ($SDGD$) [3]. For accurate edge location the error in the calculation of the zero-crossing of the $SDGD$ must be considered. Van Vliet [8] determined this error and also the error in an alternative edge location function, the Laplacian. He found that these two errors were opposite in sign and almost equal in magnitude so that adding these two functions together before finding the zero-crossing produces an error approximately one order lower than that of either method used separately. The sum of $SDGD$ and the Laplacian is called the $PLUS$ function by van Vliet and this name is used throughout this work. The $SDGD$ function is obtained from [8]

$$SDGD = \frac{B_{xx}B_x^2 + 2B_{xy}B_xB_y + B_{yy}B_y^2}{B_x^2 + B_y^2} \tag{2}$$

and the Laplacian from

$$Laplace = B_{xx} + B_{yy} \tag{3}$$

where $B_{nn} = A * G_{nn}$, $nn = x$, y, xx, yy or xy and $*$ represents convolution in the spatial domain. Here A is the image array whose Fourier transform has been band-limited by multiplying it by a low-pass Gaussian filter.

G_x and G_y are the first derivatives, with respect to x and y respectively, of a Gaussian

$$G = \frac{1}{\sqrt{2\pi}\sigma} \exp\left(- \frac{r^2}{2\sigma^2} \right), \tag{4}$$

of width σ with pixel radial location r, given by $r^2 = x^2 + y^2$ where x and y are the pixel coordinates relative to the centre of the array. G_{xx}, G_{yy} and G_{xy} are the second derivatives.

The procedure for calculating the $PLUS$ function was as follows.

1. Fourier transform the image, A, and apply a low-pass band-limiting filter.
2. Calculate the digital Gaussian filter arrays, G_{nn} and their transforms.
3. Convolve the image with the derivative arrays.
4. Inverse transform the results to produce the corresponding B_{nn} arrays.
5. Calculate the $SDGD$ and $Laplace$ arrays from Equations(2) and (3).
6. Finally, add these to produce the $PLUS$ array.

4 Zero-crossing Detection

4.1 Patch-circle Centreline Method

To locate the edge it is necessary to find the zero-crossing of the $PLUS$ function in radial directions. Since the $PLUS$ function is defined only at points on a square array, a suitable scheme has to be developed for finding the zero-crossing at subpixel locations without introducing any anisotropic distortion.

Various schemes for acquiring the $PLUS$ array point values are possible. For example, values could be taken from sections of array columns straddling a radial line, these could be interpolated to find the function value exactly on the radial line, then these new points could be interpolated to find the zero-crossing. Finding the zero-crossing this way for a series of azimuth angles produces a result similar to that shown in Fig. 1. It is clearly anisotropic.

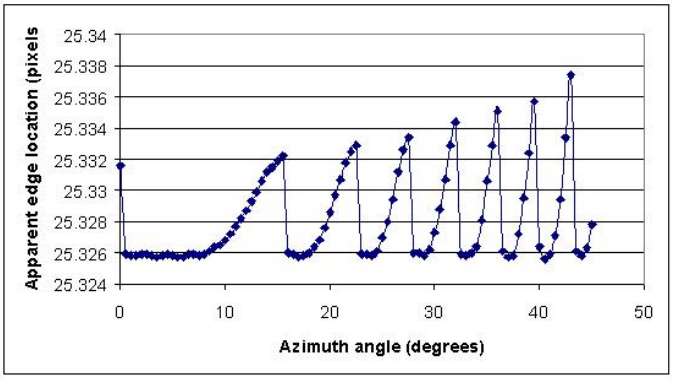

Fig. 1. Variation of apparent edge location from the zero-crossing of the $PLUS$ function showing anisotropy resulting from inappropriate spline interpolation

To avoid introducing anisotropic effects, the following scheme was adopted. Values of the $PLUS$ array were collected from points lying within a circle of a few pixels radius, centred on a point on the edge of the disc. This circle will be called the patch-circle and the geometry of the scheme is shown in Fig. 2. Let the angular position of this circle be defined by its azimuth angle, φ, the angle between a radial line through the centre of the patch-circle and the positive direction of the x-axis.

Since, for a near-circular object, the $PLUS$ function is approximately isotropic, there should be little difference in array point values for points on circumferential lines, that is, equidistant from the centre of the array if the function is correctly centred on the array. This means that all of the points within the patch-circle may be treated as if they lie on the single radial line passing through its centre. The array point values within the patch-circle then form a one-dimensional function of radius. Points were sorted in order of radius and values on pixels of common radius averaged producing a reduced set of values. This process effectively brings all points within the patch-circle to a common centreline corresponding to the azimuth angle.

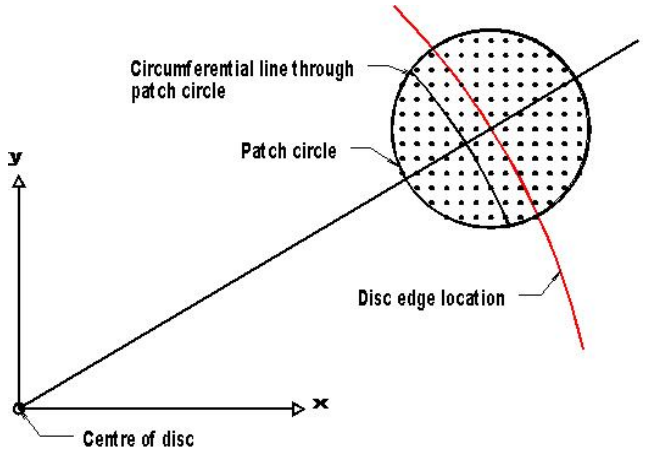

Fig. 2. Diagram showing the geometry of the patch-circle

Note that the reduced set of radii present in the patch-circle, in general, will differ for different azimuth angles (except for symmetrically 'equivalent' angles) and, furthermore, the number of radii in the set will differ also. Table 1 shows, for example, the first six radii in the reduced set for four arbitrarily chosen azimuth angles. The distribution of radii in each case is markedly different and, for angles of high symmetry with respect to the underlying array, such as $\varphi = 0$, the radii are noticeably clumped, whereas, for azimuth angles of lower symmetry, the radii are more uniformly distributed. The effect of this variation in distribution of radius with azimuth angle must be dealt with if the introduction of anisotropic effects is to be avoided. The reduced set of values must be interpolated to find

Table 1. The first six distinct pixel radii in the reduced set within the patch-circle for four arbitrary azimuth angles. The radii and number of fitted points vary with azimuth angle. Patch-circle radius 10 pixels, maximum number of points approximately 314

Azimuth Angle, φ (degrees)	0	45	21.87	-154.39
Radius	226	224.864	225.08	225.036
	226.002	225.568	225.249	225.417
	226.009	225.577	225.442	225.46
	226.02	225.595	225.462	225.524
	226.035	226.274	225.624	225.843
	227	226.279	225.657	225.854
Number of points in reduced set	169	166	313	305

an analytic form for the underlying $PLUS$ function and locate its zero-crossing. Netten [10] has investigated the types of interpolation procedure that may be used to interpolate adequately a function which has been correctly sampled and found that cubic-spline interpolation produces a satisfactory representation of the function.

A noise-free test disc of 235 pixels radius was generated in the Fourier domain as described in Section 2 and cubic-spline interpolation was used to interpolate the $PLUS$ function in the vicinity of the edge. The zero-crossing was determined in this way for every degree over 360 degrees in azimuth angle and the standard deviation found to be 1.79 x 10^{-12} pixels. Although real objects cannot be measured to this precision, it demonstrates clearly that the calculation procedure adopted effectively minimises any anisotropic effects. Note that the detected zero-crossing is independent of the number of points in the reduced set obtained from the patch-circle and is also independent of the distribution of radii as shown in the same table. Although a perfect disc has been used to establish that the calculation is effectively isotropic, the calculation procedure is ultimately intended for measurement of imperfect pipes and other curved objects.

When noise at a signal-to-noise ratio of 463 (similar to that of an x-ray CT image of a uniform object obtained using the scanner protocol specified in Section 2) was added to the computer generated disc, the standard deviation in the detected edge location over the same range of angles increased to 1.48 x 10^{-3} pixels. (Signal-to-noise ratio is here defined as the ratio of edge height grey level to standard deviation in a flat region of the disc.) Because of this marked increase in standard deviation in the presence of noise even though the underlying disc was isotropic, alternative means of determining an analytical form for the underlying $PLUS$ function were investigated.

4.2 Polynomial Fit to $PLUS$ Function (Noise-free)

The nature of the spline interpolation procedure may make the fitted function too susceptible to influence by noise, therefore, in an attempt to improve the isotropy of the edge detection procedure in the presence of noise, a single polynomial was fitted to the radial data using the Levenberg-Marquardt [11] least-squares procedure. For polynomials of order four or below, the zeros were determined analytically and for polynomials of order five or greater, an iterative polynomial solver was used to find the zeros [11], one of which represents the actual zero-crossing of the $PLUS$ function. Polynomials of odd order from 3 to 11 were fitted and the standard deviations in apparent zero-crossing were measured over all angles as above. The results are shown in the second column of Table 2 for a noise-free disc.

Note that the isotropy is nowhere near as good as it was when using cubic spline interpolation (last column) even for orders as high as eleven. The anisotropy in this case is caused by model error. There is no stochastic error because the test disc is noise-free. The model error occurs because even an eleventh order polynomial is unable to represent accurately the form of the

Table 2. Standard deviation in zero-crossing (pixels) at one degree intervals over 360 degrees azimuth angle as a function of fit order using polynomial fit, Chebyshev approximation (and cubic spline interpolation)

Fit Order	Polynomial fit	Chebyshev Approximation	Cubic Spline Interpolation
-	-	-	1.79×10^{-12}
3	3.44×10^{-5}	3.44×10^{-5}	-
5	2.34×10^{-7}	2.34×10^{-7}	-
7	4.04×10^{-8}	1.60×10^{-9}	-
9	7.73×10^{-8}	9.40×10^{-12}	-
11	1.12×10^{-7}	4.82×10^{-12}	-

$PLUS$ function. Although precision of the order 10^{-12} is not required for industrial measurements, it is important to ensure that the measurement process is not contributing anisotropic effects to the apparent zero-crossing. The combined effect of the model error and the variation in distribution of radii in the reduced set produces a slightly different fit at each angle and hence a small variation in detected zero-crossing.

4.3 Chebyshev Approximation to *PLUS* Function (Noise-free)

To minimise this variation in fit with azimuth angle, a model with a better fit to the underlying $PLUS$ function was required. A Chebyshev approximation [12] was used for this purpose because the convergence is generally much faster than similar series approximations such as Taylor series and a much better fit can be obtained at a given order than a conventional polynomial of the same order. The Chebyshev approximation was implemented using the same least-squares procedure as for the polynomial fit above. To find the zero-crossing after the fitted coefficients were determined, the Chebyshev polynomials were solved using the same iterative polynomial solver as before. Chebyshev polynomials of odd orders 3 to 11 were fitted to the noise-free $PLUS$ function and the standard deviation in zero-crossing measured over all angles for each order. The results are also shown in column 3 of Table 2 for comparison with the results of the polynomial fits in column 2.

For third and fifth orders, the angular variation is the same for both polynomial fit and Chebyshev approximation. However, for seventh order and above, the angular variation using the Chebyshev approximation becomes rapidly better than the variation with the polynomial fit and for ninth and eleventh orders, the Chebyshev approximation produces a variation of the order 10^{-12} pixels, approximately four orders of magnitude lower than the corresponding polynomial fit and comparable with the cubic spline interpolation. It is evident that there is not much to be gained by using Chebyshev approximation orders higher than about the ninth.

5 Analysis of Fourier Disc with Noise and Experimental X-ray Data

Having established that the Chebyshev approximation to the PLUS function permits zero-crossing detection with negligible anisotropy in the case of noise-free Fourier discs, noise was added to the same disc in the manner described in Section 2.

The zero-crossing of the $PLUS$ function was again detected at one degree intervals over 360 degrees as described above for the odd orders of conventional and Chebyshev polynomials between 3 and 11 and for cubic spline interpolation. The all-angle standard deviations were found to be virtually equal over all orders for both polynomial and Chebyshev fits. The results for the eleventh order Chebyshev approximation are shown in Table 3. The standard deviation for the eleventh order Chebyshev approximation was approximately 11 to 12 percent lower than the cubic spline interpolation for the computer generated discs investigated. The preliminary x-ray CT measurement is shown in the same table and the result is appreciably higher due to variation in apparent disc centre location between projections.

Table 3. Standard deviation in zero-crossing (pixels) at one degree intervals over 360 degrees azimuth angle for noise-free and noise-added disc images using cubic spline interpolation and Chebyshev approximation. X-ray result calculated at two degree intervals

Disc	Noise-free	463 SNR	X-ray CT
Cubic spline	1.79×10^{-12}	1.48×10^{-3}	-
Chebyshev (11th order)	4.82×10^{-12}	1.32×10^{-3}	3.5×10^{-2}

6 Conclusion

In making accurate subpixel measurements from images of objects with approximately circular symmetry, there are various sources of discrete pixel anisotropy which need to be allowed for if measurement errors are to be avoided. This is true even for a properly sampled and band-limited image function of perfect circular symmetry because of the lattice of sample points.

A satisfactory way of accurately measuring the edge location of such objects without introducing anisotropic effects is to find the zero-crossing of van Vliet's PLUS function using the 'patch-circle centreline' method described above.

For noise-free images, cubic spline interpolation, or alternatively 9th order Chebyshev approximation, to the $PLUS$ function reduce the circumferential variation in apparent edge location around the circle to a standard deviation of

approximately 10^{-12} pixels for a disc radius of approximately 235 pixels. Ninth order polynomial fitting to the $PLUS$ function, however, produces a circumferential variation about four orders of magnitude higher because of the combined effect of model error in the fitting function and variation with azimuth angle of the distribution of the independent variable of the data to be fitted. Measurement of computer generated disc images with noise and x-ray images have been measured to precisions of 1.3 x 10^{-3} and 3.5 x 10^{-2} pixels respectively. Work on the latter is continuing.

Acknowledgements

RBH wishes to thank Monash University for the provision of a Monash Graduate Scholarship and gratefully acknowledges discussions with Dr L.J. van Vliet and colleagues of the Faculty of Applied Physics, Delft University of Technology, The Netherlands.

References

1. Porter, J.B.: On Line Controls. Proc. SME Medical Tubing Technology Seminar, (1995), Revised August, (1999)
2. Onel, Y., Ewert, U., Willems, P.: Radiographic Wall Thickness Measurement of Pipes by a New Tomographic Algorithm. 15th World Congress on NDT, Rome, (2000)
3. Gonzalez, R.C., Woods, R.E.: Digital Image Processing. 2nd edn. Prentice Hall, New Jersey (2002)
4. Tabatabai, A.J.,Mitchell, O.R.: Edge Location to Subpixel Values in Digital Imagery. IEEE Trans. Pattern Anal. Machine Intell. **PAMI-6** (1984) 188–201
5. Huertas, A., Medioni, G.: Detection of Intensity Changes with Subpixel Accuracy Using Laplacian-Gaussian Masks. IEEE Trans. Pattern Anal. Machine Intell. **PAMI-8** (1986) 651–664
6. Lyvers, E.P., Mitchell, O.R., Akey, M.L., Reeves, A.P.: Subpixel Measurements Using a Moment-Based Edge Operator. IEEE Trans. Pattern Anal. Machine Intell. **PAMI-11** (1989) 1293–1309
7. Chen, F-L., Lin, S-W: Subpixel Estimation of Circle Parameters Using Orthogonal Circular Detector. Computer Vision and Image Understanding **78** (2000) 206–221
8. van Vliet, L.J.: Grey-Scale Measurements in Multi-Dimensional Digitized Images. Ph.D. Thesis, Delft University Press, Stevinweg 1, Delft, The Netherlands, (1993).
9. Verbeek, P.W., van Vliet, L.J.: On the Location Error of Curved Edges in Low-Pass Filtered 2-D and 3-D Images. IEEE Trans. Pattern Anal. Machine Intell. **PAMI-16** (1994) 726–733
10. Netten, H.: Exact Reconstruction of Sampled Images. M.Sc. Thesis, Pattern Recognition Group, Faculty of Applied Physics, Delft University of Technology, The Netherlands, (1990)
11. GNU Scientific Library – Reference Manual.
12. Fox, L., Parker, I.B.: Chebyshev Polynomials in Numerical Analysis. Oxford University Press, London, New York (1968)